




Open Access Article

 <https://doi.org/10.35741/issn.0258-2724.59.1.15>

Research article

Materials Science

## FABRICATION AND MECHANICAL CHARACTERIZATION OF TiSiN, DLC, AND TiSiN/DLC COATINGS DEPOSITED BY THE FILTERED CATHODIC ARC TECHNIQUE

### 通过过滤阴极电弧技术沉积的泰信、DLC和钛辛/DLC涂层的制造和机械特性

Apithan Kitjindarnon<sup>a</sup>, Nuntapol Vattanaprteep<sup>a</sup>, Nurot Panich<sup>b</sup>, Prayoon Surin<sup>a\*</sup>

<sup>a</sup>Department of Advanced Manufacturing Technology, Faculty of Engineering, Pathumwan Institute of Technology Bangkok, Thailand, [6512223103@pit.ac.th](mailto:6512223103@pit.ac.th), [6512313101@pit.ac.th](mailto:6512313101@pit.ac.th), [Prayoon@pit.ac.th](mailto:Prayoon@pit.ac.th)

<sup>b</sup>Faculty of Engineering, Rajapark Institute Bangkok, Thailand, [nurotw@yahoo.com](mailto:nurotw@yahoo.com)

\* Corresponding author: [Prayoon@pit.ac.th](mailto:Prayoon@pit.ac.th).

Received: December 23, 2023 ▪ Reviewed: January 14, 2024  
Accepted: February 11, 2024 ▪ Published: February 29, 2024

#### Abstract

This research studied the fabrication and characterization of intrinsic mechanical properties of resultant TiSiN, DLC (low-normal-high voltage bias), and TiSiN/DLC coatings deposited by the filtered cathodic arc technique. The morphology, structural, and mechanical properties of the resulting coatings were examined and characterized by conventional SEM, AFM, XRD, nanoindentation, and micro-scratch approaches. The experimental results show that all coatings can achieve very high hardness and good adhesion. TiSiN emerges as the most promising coating, demonstrating superior mechanical properties such as high hardness as a superhard coating, high elastic modulus, and high critical load to the coating failure ( $L_c$ ). The preferred (111) orientation can be found in all coatings, resulting in high hardness and adhesion. For DLC coatings, the increment of bias voltage is affected to enhance the mechanical properties. The deposition process could be controlled to produce a hybrid TiSiN/DLC coating with both high hardness and good adhesion strength, demonstrating the advantages of combining TiSiN and DLC. The overall mechanical performance attests to viability of the application of advanced coatings with enhanced mechanical resilience.

**Keywords:** titanium silicon nitride coatings, diamond-like carbon coatings, titanium silicon nitride/diamond-like carbon coatings, mechanical properties



**摘要** 本研究研究了通过过滤阴极电弧技术沉积的氮化钛、DLC（低-正常-高电压偏置）和氮化钛/DLC涂层的制造和固有机械性能表征。通过传统的扫描电镜、原子力显微镜、X射线衍射、纳米压痕和微划痕方法对所得涂层的形态、结构和机械性能进行了检查和表征。实验结果表明，所有涂层都能达到非常高的硬度和良好的附着力。氮化钛成为最有前途的涂层，表现出优异的机械性能，例如超硬涂层的高硬度、高弹性模量和涂层失效的高临界载荷(Lc)。所有涂层均具有优选的(111)取向，从而具有高硬度和附着力。对于DLC涂层，通过影响偏置电压的增量来增强机械性能。可以控制沉积过程以产生具有高硬度和良好附着强度的混合氮化钛/DLC涂层，展示了氮化钛和DLC结合的优势。整体机械性能证明了具有增强机械弹性的先进涂层应用的可行性。

**关键词:** 氮化钛硅涂层、类金刚石碳涂层、氮化钛硅/类金刚石碳涂层、机械性能

## I. INTRODUCTION

Generally speaking, a hard coating applied to the surface of another material plays a major role in enhancing its durability, scratch resistance, and improved performance, such as mechanical properties [1-3]. There are many applications for thin, hard, protective, and wear-resistant coatings in metal cutting tools. The invention of low-temperature physical vapor deposition (PVD) techniques such as cathodic arc has made the deposition of various hard, protective, and wear-resistant coatings to commercial substrate tool steel promising. The aim of expanding the tool lifetime can be achieved by applying appropriate deposition approaches with deposition conditions.

In the process of coating materials selection, titanium silicon nitride (TiSiN) and diamond-like carbon (DLC) were specifically chosen. Both TiSiN and DLC are commonly studied with actual uses in commercial markets because they possess many interesting physical, mechanical, and chemical properties, such as high hardness, good elastic modulus, and low coefficient of friction. Currently, material processing tools and

dies industries acknowledge that the coating method can help to reduce lost due to wear and corrosion in engineering components [4-6]. The quest of finding the optimization of coating parameters will be studied to achieve both high hardness and modulus and the tribological and corrosion properties.

In this investigation, attempts were made to fabricate TiSiN, DLC (low, normal, and high voltage bias), and TiSiN/DLC coatings on tungsten carbide tool steel substrate under various controlled parameters. Characterization of the structures and mechanical properties of the resultant coatings was carried out.

## II. EXPERIMENTAL PROCEDURE

In this study, the tungsten carbide (WC) tool steel substrate was chosen. The specimen surface was manually ground and polished. The WC substrates were then ultrasonically cleaned with acetone and ethanol before being charged into the deposition chamber. A cathodic arc system supplied by Diacoat Technologies Co., Ltd. was used for deposition, as shown in Figure 1.



Figure 1. (a) TiSiN, (b) low DLC, (c) normal DLC, (d) high DLC, and (e) TiSiN/DLC coatings on tungsten carbide (Developed by the authors)

The system consists of a cylindrical chamber with three 4-inch water-cooled target holders tilted at approximately 30 degree with respect to the normal of the horizontal substrate holder, which can be heated by graphite heating elements. All the experiments were conducted at a constant working pressure of 0.65 Pa and a total gas flow rate (Ar) of 20 sccm. The substrate

temperature can be changed from room temperature (RT) until 480°C. An RF power biased to the substrate was used to sputter clean the substrate surface.

For the TiSiN coatings, the deposition of a pure Ti layer was conducted for 5 min at a bias voltage of the substrate of -200 V and a Ti cathode current of 120 to 140 A. The TiSiN top

layer was deposited for 90 min using a TiSi cathode with an arc current of 120–140 A and bias between 8 and 130 A. During all deposition steps, the substrate was rotated, and the rotating speed of the samples was set to 20 rpm. The substrate coating temperature at 480°C.

DLC and TiSiN/DLC coatings were fabricated using the filtered cathodic vacuum arc (FCVA), as shown in Figure 2. The Ti interlayer was sputtered using DC magnetron sputtering with the substrate temperature at 170°C. The substrate-to-Ti target distance was 80 mm. The vacuum chamber is evacuated to a base pressure of  $3.0 \times 10^{-3}$  Pa. The substrates were etched for 20 min in Ar ions. The cathodes were operated using a DC arc current of 60 to 100 A. Three different DC bias voltages from -1000 to -2000 V were introduced during deposition: low bias at -1000 V, normal bias at -1500 to -1700 V, and high bias at -1900 to -2000 V.

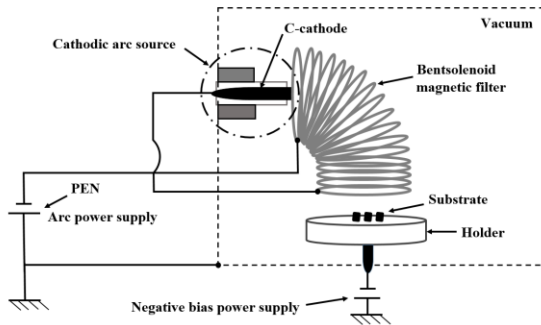
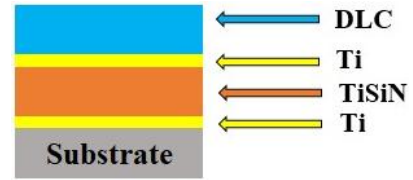
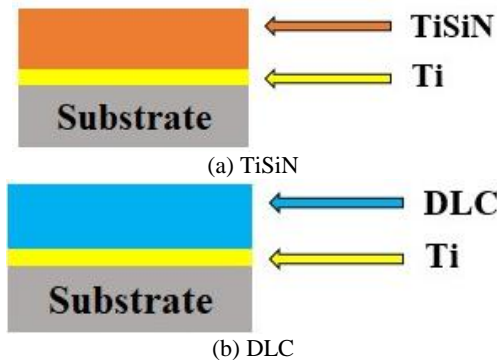


Figure 2. Schematic of the filtered cathodic vacuum arc (FCVA) coating deposition process (Developed by the authors)

The experiments were conducted to study the effect of various parameters on the structure and properties of TiSiN, DLC, and TiSiN/DLC coatings with a Ti interlayer. The purpose of depositing a thin Ti interfacial layer by sputtering a pure Ti target for a few minutes is to increase the adhesion between the WC substrate and top coating, as shown in Figure 3.



(c) TiSiN/DLC

Figure 3. Schematic of the TiSiN, DLC, and TiSiN/DLC coatings (Developed by the authors)

The phase identification of the resultant coatings was examined using a Rigaku X-ray diffractometer (Miniflex 2). Scanning electron microscopy (SEM, Quanta 450) and energy dispersive spectroscopy were conducted by Oxford INCA-350. The coating thickness was measured by making a ball crater on the coating surface using a Calotest machine manufactured by Anton Paar. The roughness of the surfaces was imaged using atomic force microscopy (AFM). The indentation test was performed using a nanoindentation test using the Fischer HM2000 model. The micro-scratch test was performed using the single-pass scratch mode with micro-scratch using the Fischer ST200 model, as shown in Figure 4.

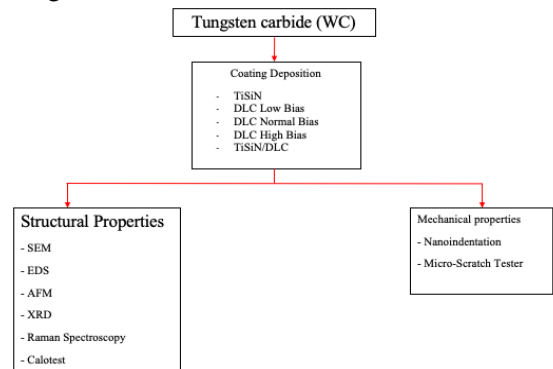


Figure 4. Flow diagram of TiSiN, DLC (low, normal and high bias), and TiSiN/DLC coating characterization (Developed by the authors)

### III. RESULTS AND DISCUSSION

#### A. Structural Characterization

Table 1 summarizes the properties of the resultant coatings. X-ray diffraction analysis (Figure 5) shows that all the TiSiN, DLC, and TiSiN/DLC coatings exhibit broad diffraction peaks corresponding to the TiSiN, DLC, and TiSiN/DLC phases, irrespective of the deposition temperature. Small peaks of Ti were also found, as expected, which are from the Ti interlayer. The presence of a single peak suggests a fiber texture with preferred (111), (110), and (200) orientations in the TiSiN coatings.

Table 1. Summary of the resultant coating properties (Developed by the authors)

Coatings Material	Coating Thickness ( $\mu\text{m}$ )	Roughness RMS (nm)	Coating Texture	Hardness (GPa)	Elastic Modulus (GPa)	Critical Load (mN)
TiSiN	1.56	46.07	(111), (110), (200)	40.9	362	80.66
DLC (Low Bias)	1.02	9.17	(111), (110)	31.8	335	42.99
DLC (Normal Bias)	1.02	8.10	(111), (110)	34.2	294	50.19
DLC (High Bias)	1.03	9.97	(111), (110)	36.0	333	41.27
TiSiN/DLC	1.77	36.74	(111), (110), (200)	36.2	320	55.80

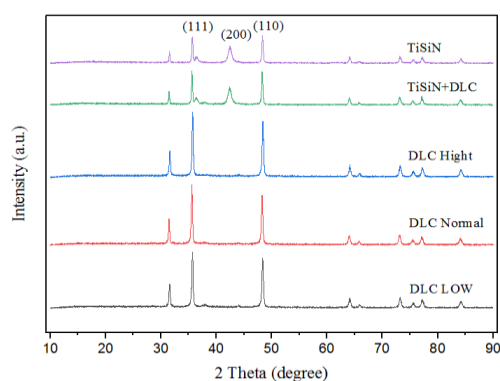
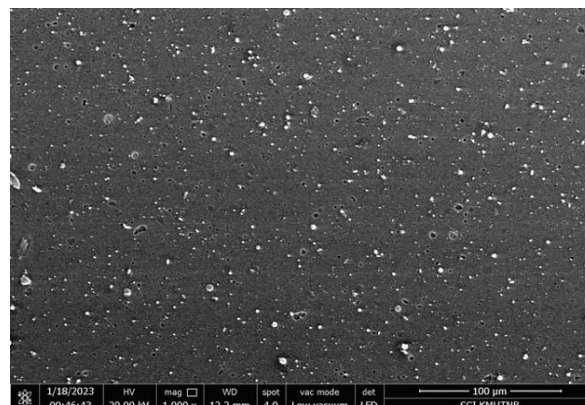


Figure 5. XRD patterns generated from TiSiN, DLC, and TiSiN/DLC coatings with a Ti interlayer (Developed by the authors)

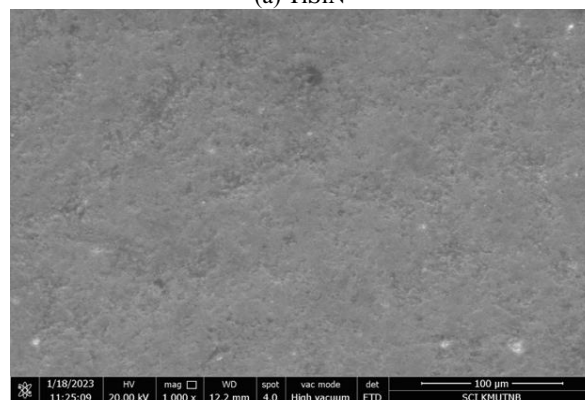
From the literature, most of the reported TiSiN coatings display patterns of the hexagonal phase with a preferred (111) orientation [7, 8], and the (111)-oriented coatings yield the highest hardness [8, 9]. This is the same pattern as DLC. Since the (111) plane has the highest packing factor, energetic adatoms are required to create such an orientation. To enhance the development of the desired (111) orientation for DLC, 3 different biasing powers were studied.

It was found that the higher the biasing power, the more the desired (111) orientation, as shown in Figure 5.

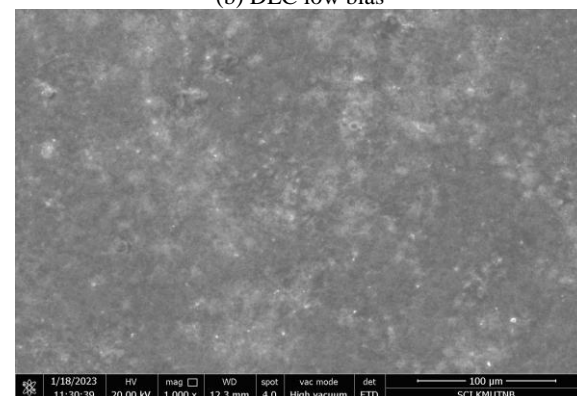
The coating morphology was studied. Figure 6 shows the morphology of (a) TiSiN, (b) low DLC, (c) normal DLC, (d) high DLC, and (e) TiSiN/DLC coatings. It can be seen that the surface morphology of the TiSiN film showed several macro-particles, whereas the surface morphology of the DLC film was much smoother and less porous than TiSiN, resulting in the roughness of the resultant coatings summarized in Table 1.



(a) TiSiN



(b) DLC low bias



(c) DLC normal bias

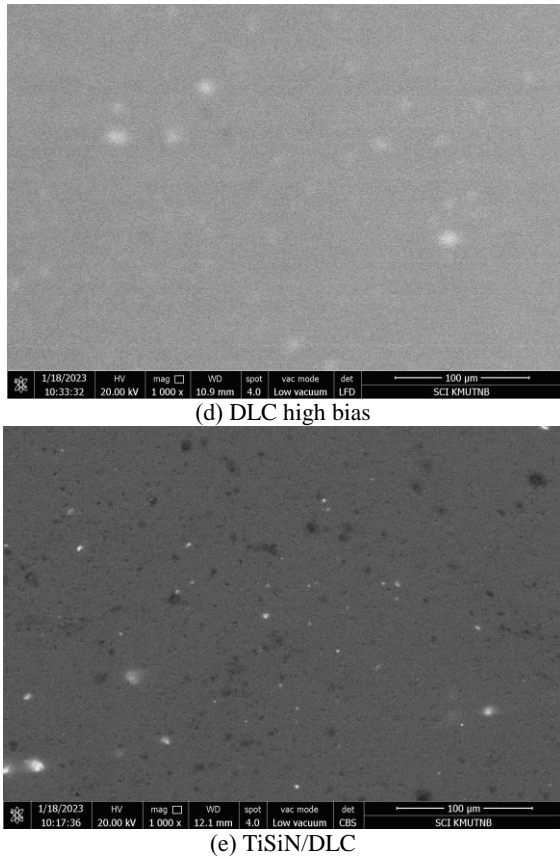


Figure 6. SEM of the morphology of (a) TiSiN, (b) low DLC, (c) normal DLC, (d) high DLC, and (e) TiSiN/DLC coatings (Developed by the authors)

The AFM images of the morphology of the TiSiN and DLC coatings in Figure 7 confirm the structure of the populated coating. Although TiSiN has a higher value of surface roughness, the AFM image shows a dense morphology, which resulted in super high hardness compared to DLC, as shown in Table 1.

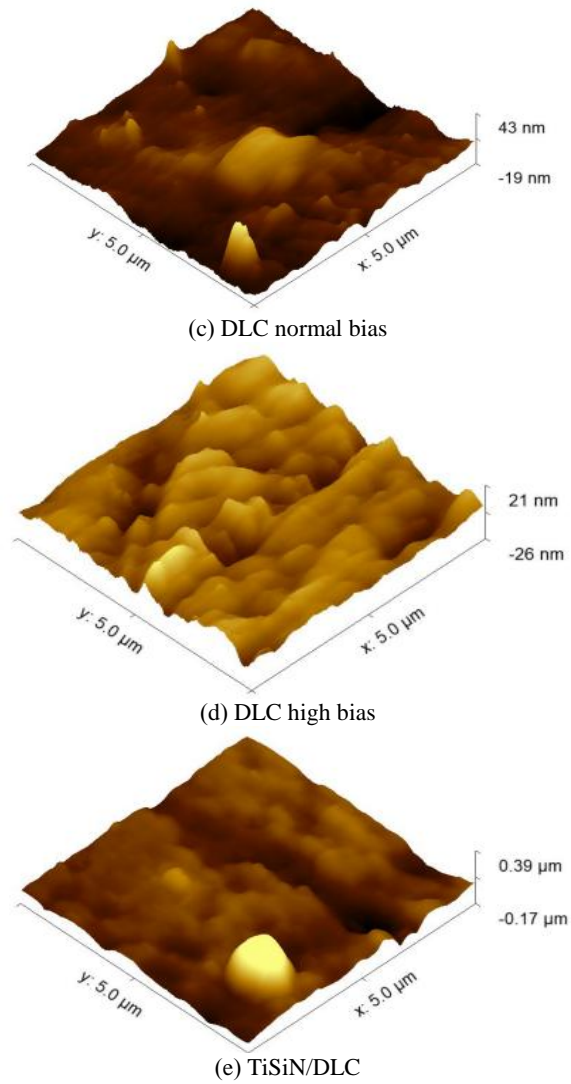
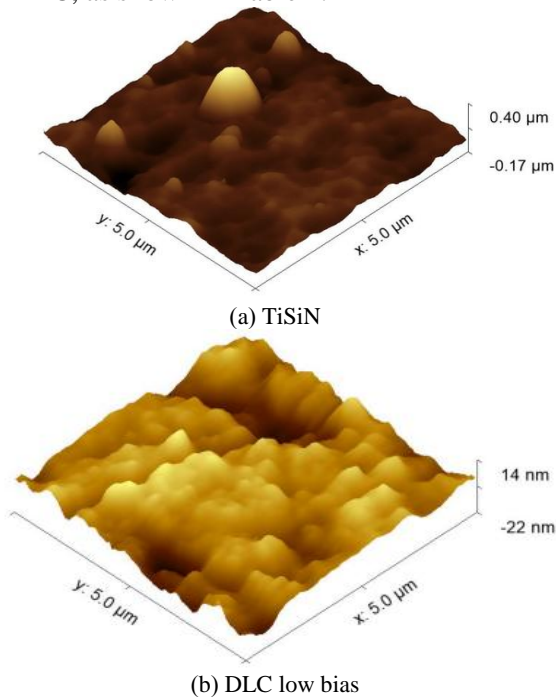


Figure 7. AFM of the morphology of (a) TiSiN, (b) low DLC, (c) normal DLC, (d) high DLC, and (e) TiSiN/DLC coatings (Developed by the authors)

## B. Coating Properties

### 1) Nanoindentation Test

The mechanical properties of the thin film/coatings, such as hardness, were examined using a conventional indentation technique so that the intrinsic mechanical properties of the coating could be achieved. Figure 8 shows the relationship between the load applied and the indentation depth of the coatings. Although indentation was tested at various indentation depths, due to the thin coating thickness (Table 1) and the substrate effect exclusion, the hardness and elastic modulus values summarized in Table 1 were achieved from a 100-nm depth for all tests. It can be seen that the TiSiN coatings with (111) orientations exhibit hardness and modulus values higher than those reported by other investigators [10]. The DLC coatings with (111) orientations also exhibit hardness and modulus values. The hardness and modulus values of the resultant coatings are presented in Figure 9. For DLC coatings, it can be seen that a higher biasing

power promotes higher hardness and modulus values. This low hardness achieved from the low biasing power is due to the poor orientation, small thickness, and poor adhesion of the coating.

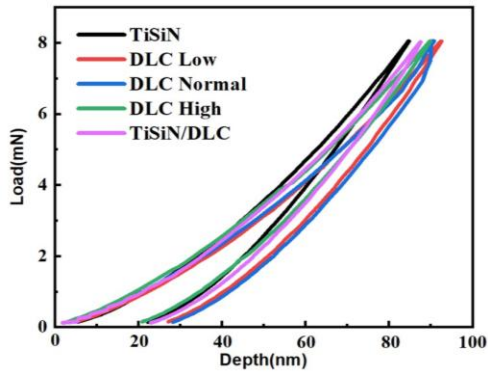


Figure 8. Load-displacement curves of the resultant coatings (Developed by the authors)

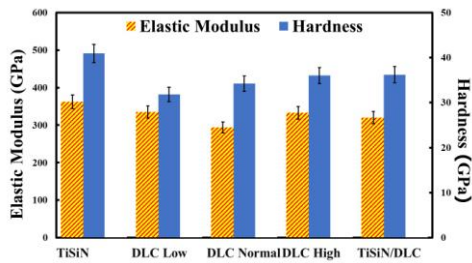
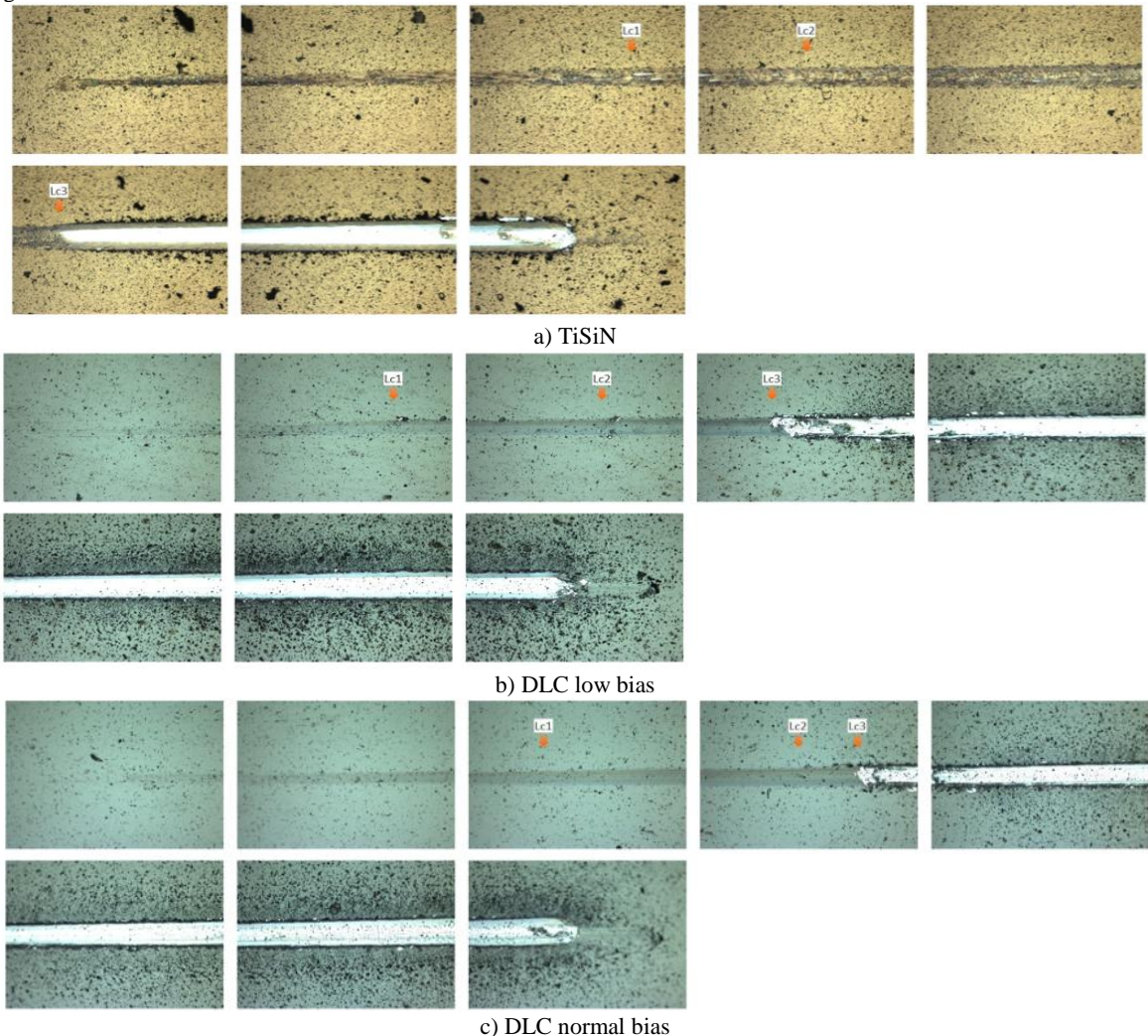


Figure 9. Hardness and elastic modulus of the resultant



coatings (Developed by the authors)

2) *Micro-Scratch Test*

Coating adhesion was tested using a conventional micro-scratch adhesion test. This scratch technique is commonly used to find and evaluate the critical load for coating failure ( $L_c$ ) by plotting friction force against load. Optical microscopic examinations were also used to confirm the results from the friction curve. The results are summarized in Table 1.

As expected, because all DLC coatings have a very thin coating thickness, adhesive failure could be found easier compared to TiSiN and TiSiN/DLC coatings. The critical load,  $L_c$ , for adhesive failure of these DLC coatings was found to be low, in the range of 41–50 mN (Table 1). No correlation was found between  $L_c$  and biasing power. Figure 10 shows typical scratch tracks measured by optical microscopy, in which the mechanism of coating failure can be observed. From Table 1, it can be seen that the critical load was measured to be 80.66 mN in the TiSiN coatings, which also exhibit the highest hardness and modulus.

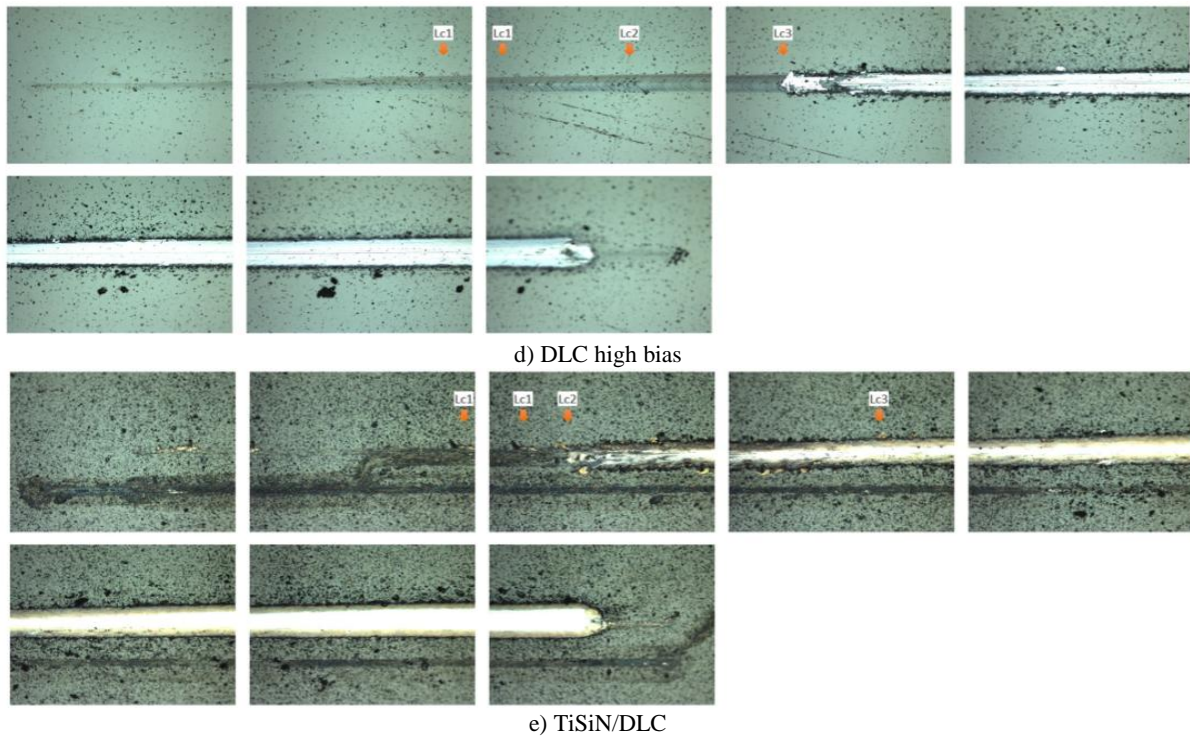


Figure 10. Optical images of the scratch test of TiSiN/DLC coatings (Developed by the authors)

#### IV. CONCLUSION

Based on the experiments, the main results are summarized as follows:

(1) TiSiN, DLC (low, normal and high bias), and TiSiN/DLC hybrid coatings can be produced by the filtered cathodic arc technique, showing (111) orientations and having high hardness and adhesion with the substrate.

(2) The fabrication of a super-hard coating at 40.9 GPa for a TiSiN coating can be achieved by optimizing the coating conditions.

(3) The hardness and elastic modulus of DLC coatings are significantly affected by the biasing power during deposition, and a higher biasing power provides higher hardness and modulus.

(4) The biasing power does not affect adhesion with the substrate.

(5) The deposition process could be optimized to fabricate TiSiN/DLC coatings with high hardness and good adhesion strength.

#### ACKNOWLEDGMENT

The authors would like to thank Diacoat Technologies Co., Ltd. of Thailand for technological assistance in producing the coating.

#### DECLARATIONS

#### Author Contributions

Conceptualization, A.K.; methodology, N.V.; validation, N.P.; formal analysis, P.S.;

investigation, N.P.; resources, N.V.; data curation, P.S.; writing—original draft preparation, N.P.; writing—review and editing, N.V.; visualization, P.S.; supervision, A.K.; project administration, A.K. All authors have read and agreed to the published version of the manuscript.

#### Data Availability Statement

The data presented in this study are available on request from the corresponding author.

#### Conflicts of Interest

The authors declare no conflict of interest.

#### REFERENCES

- [1] MORITZ, Y., KAINZ, C., TKADLETZ, M., CZETTL, C., POHLER, M., and SCHALK, N. (2021) Microstructure and mechanical properties of arc evaporated Ti(Al,Si)N coatings. *Surface and Coatings Technology*, 421, 12746.
- [2] CHANG, Y.-Y., YANG, Y.-J., and WENG, S.-Y. (2020) Effect of interlayer design on the mechanical properties of AlTiCrN and multilayered AlTiCrN/TiSiN hard coatings. *Surface and Coatings Technology*, 389, 125637.

- [3] ZIBEROV, M., DE OLIVEIRA, D., DA SILVA, M.B., and HUNG, W.N.P. (2020) Wear of TiAlN and DLC coated microtools in micromilling of Ti-6Al-4V alloy. *Journal of Manufacturing Processes*, 56, pp. 337–349.
- [4] MOVASSAGH-ALANAGH, F. and MAHDAVI, M. (2020) Improving wear and corrosion resistance of AISI 304 stainless steel by a multilayered nanocomposite Ti/TiN/TiSiN coating. *Surfaces and Interfaces*, 18, 100428.
- [5] MARCHIN, N. and ASHRAFIZADEH, F. (2021) Effect of carbon addition on tribological performance of TiSiN coatings produced by cathodic arc physical vapour deposition. *Surface and Coatings Technology*, 407, 126781.
- [6] WANG, D., GONG, Z., JIANG, B., YU, G., LIU, G., and WANG, N. (2020) Structure original of temperature depended superlow friction behavior of diamond like carbon. *Diamond and Related Materials*, 107, 107880.
- [7] GENG, D., ZENG, R., WU, Z., and WANG, Q. (2020) An investigation on microstructure and milling performance of arc-evaporated TiSiN/AlTiN film. *Thin Solid Films*, 709, 138243.
- [8] AKHTER, R., ZHOU, Z., XIE, Z., and MUNROE, P. (2021) Influence of substrate bias on the scratch, wear and indentation response of TiSiN nanocomposite coatings. *Surface and Coatings Technology*, 425, 127687.
- [9] AKHTER, R., ZHOU, Z., XIE, Z., and MUNROE, P. (2021) TiN versus TiSiN coatings in indentation, scratch and wear setting. *Applied Surface Science*, 563, 150356.
- [10] BAI, X., LI, J., and ZHU, L. (2019) Structure and properties of TiSiN/Cu multilayer coatings deposited on Ti6Al4V prepared by arc ion plating. *Surface and Coatings Technology*, 372, pp. 16-25.
- 能涂料。表面和涂层技术, 421, 12746。
- [2] 张Y.-Y., 杨Y.-J., 翁S.-Y. (2020) 夹层设计对铝钛铬氮化物和多层氮化铝钛铬/氮化硅钛硬质涂层机械性能的影响。表面和涂层技术, 389, 125637。
- [3] ZIBEROV, M., DE OLIVEIRA, D., DA SILVA, M.B. 和 HUNG, W.N.P. (2020) Ti-6Al-4V合金微铣削中氮化钛和DLC涂层微型刀具的磨损。制造工艺杂志, 56, 第 337-349 页。
- [4] MOVASSAGH-ALANAGH, F. 和 MAHDAVI, M. (2020) 通过多层纳米复合钛/氮化钛/氮化硅涂层提高美国钢铁协会304不锈钢的耐磨性和耐腐蚀性。表面和界面, 18, 100428。
- [5] MARCHIN, N. 和 ASHRAFIZADEH, F. (2021) 碳添加对阴极电弧物理气相沉积生产的氮化钛涂层摩擦学性能的影响。表面和涂层技术, 407, 126781。
- [6] 王丹, 龚正, 姜波, 余光, 刘光, 王娜 (2020) 类金刚石碳超低摩擦温度依赖行为的结构原始。金刚石及相关材料, 107, 107880。
- [7] 耿大., 曾瑞., 吴志., 王强. (2020) 电弧蒸发氮化钛/氮化铝薄膜的微观结构和铣削性能研究。固体薄膜, 709, 138243。
- [8] AKHTER, R., ZHOU, Z., XIE, Z. 和 MUNROE, P. (2021) 基材偏差对氮化钛纳米复合涂层划痕、磨损和压痕响应的影响。表面和涂层技术, 425, 127687。
- [9] AKHTER, R., ZHOU, Z., XIE, Z. 和 MUNROE, P. (2021) 锡与氮化钛涂层在压痕、划痕和磨损设置中的比较。应用表面科学, 563, 150356。
- [10] BAI, X., LI, J., 和 ZHU, L. (2019) 电弧离子镀钛6铝4V上沉积的氮化钛/铜多层涂层的结构和性能。表面和涂层技术, 372, 第 16-25 页。

#### 参考文献:

- [1] MORITZ, Y., KAINZ, C., TKADLETZ, M., CZETTL, C., POHLER, M., 和 SCHALK, N. (2021) 电弧蒸发钛(铝,硅)氮的微观结构和机械性